J. Phys. B: At. Mol. Opt. Phys. **42** (2009) 215307 (11pp) doi:10.1088/0953-4075/42/21/215307

Characteristic oscillations in the coherent transients of ultracold rubidium molecules using red and blue detuned pulses for photoassociation

Fabian Weise[1], Andrea Merli[1], Frauke Eimer[1], Sascha Birkner[1], Franziska Sauer[1], Ludger Wöste[1], Albrecht Lindinger[1], Wenzel Salzmann[2], Terence G Mullins[2], Roland Wester[2], Matthias Weidemüller[3], Ruzin Ağanoğlu[4] and Christiane P Koch[4]

[1] Institut für Experimentalphysik, Freie Universität Berlin, Arnimallee 14, D-14195 Berlin, Germany
[2] Physikalisches Institut, Universität Freiburg, Hermann Herder Str 3, D-79104 Freiburg i. Br., Germany
[3] Physikalisches Institut, Ruprecht-Karls-Universität Heidelberg, Philosophenweg 12, D-69120 Heidelberg, Germany
[4] Institut für Theoretische Physik, Freie Universität Berlin, Arnimallee 14, D-14195 Berlin, Germany

E-mail: weise@physik.fu-berlin.de

Received 4 August 2009, in final form 23 September 2009
Published 27 October 2009
Online at stacks.iop.org/JPhysB/42/215307

Abstract
We investigate the interaction of femtosecond laser pulses with an ensemble of ultracold rubidium atoms by applying shaped excitation pulses with two different types of spectral filtering. Although the pulses, which are frequency filtered with a high pass, have no spectral overlap with molecular states, we observe coherent molecular transients. Similar transients obtained with nearly transform-limited pulses, where only the atomic resonance is removed, reveal two differing oscillatory components. The resulting transients are compared among themselves and supported with quantum dynamical simulations which indicate a photoassociation process. The effect is due to the strong field interaction of the pulse with the colliding atom pair.

(Some figures in this article are in colour only in the electronic version)

1. Introduction

The invention of cooling and trapping of atoms to the point of Bose–Einstein condensation had an enormous impact on the field of atomic physics [1]. In ultracold gases, where the de Broglie wavelength is in the range of the interparticle distance, quantum effects become accessible. Many different fields of physics benefit from the availability of samples of dense ultracold gases. For instance, collision experiments, quantum computing, testing of fundamental physical constants and high-precision measurements in metrology become feasible [2]. Extending the ultracold samples to molecules will have further interesting prospects.

Because of the internal degrees of freedom, it is not possible to apply the same cooling techniques to molecules and different approaches are required. Buffer gas cooling [3] and Stark decelerators [4] can produce molecules with temperatures of a few millikelvin. However, lower temperatures cannot be achieved with these direct cooling methods. Alternatively, molecules can be produced, starting from an ensemble of cold atoms. Nowadays, magnetic association using Feshbach resonances [5] or photoassociation [6] with narrow band cw lasers are common techniques.

Recently, the investigation and manipulation of ultracold gases with ultrashort laser pulses, in particular with the goal of photoassociation, have become a hot topic. Many theoretical proposals predict higher photoassociation efficiencies [7] and

the potential to create ground-state molecules [8] and to stabilize them [9] with the help of pulsed lasers. Because of their broad band frequency spectrum, laser pulses excite several vibrational states and therefore offer more possibilities for control than cw laser light. With the well-established experimental techniques of pulse shaping and feedback loop optimization it became possible to control molecular wavepacket dynamics and drive them to desired states [10]. Over the last decade, this has been successfully applied to many different problems such as multi-photon transitions [11], selective bond breaking [12], isomerization [13] and many more. Inspired by the theoretical proposals a growing number of coherent control experiments on ultracold gases are being carried out. Attempts to control molecular formation started with pulses of picosecond [14] and nanosecond [15] duration. The first experiments on ultracold molecules using femtosecond (fs) laser pulses investigated the suppression of photoassociation by applying a chirp [16] or closed feedback loop optimization [17]. Further work, in which coherent control techniques have been successfully applied on ultracold molecules, includes the optimization of multi-photon ionization of ultracold Rb_2 [18] and cooling of molecules to the vibrational ground state [19, 20].

Lately, we have presented the transients of two colour femtosecond pump probe measurements [21] which reveal the first indication for femtosecond photoassociation. In this experiment, a fs laser pulse which is frequency modulated by a sharp low-pass filter creates population in the molecular first excited state. This population is ionized by a subsequent probe pulse applied with variable time delay. The transients resulting from different cut-off positions as well as the effect of spectral phases are reproduced by corresponding quantum dynamical simulations. Along with further measurements their analysis indicates the photoassociation of two colliding atoms into a molecule by the pump pulse [22, 23]. Recently, a similar experiment has investigated this process on a longer time scale [24].

In all these experiments, the transients were investigated by using frequency modulated femtosecond laser pulses for photoassociation which have their frequencies red detuned to the atomic resonance. Measurements using spectrally very narrow pulses have revealed that the frequencies driving the photoassociation process are those which are very close to the atomic resonance [25].

The photoassociation is due to off-resonant strong field excitation [21]. Therefore the blue components, which have not been studied so far, are also expected to contribute to this process. Here, the effect of pulses which have their spectral intensity blue detuned to the atomic resonance on the photoassociation process and its transients are investigated. In principle pulses, which provide both red and blue detuned frequencies, should offer a greater possibility for control of this strong field effect for instance by interferences. This is experimentally and theoretically investigated with a second type of pulses which make use of the frequencies red and blue detuned to the atomic resonance. In these pulses, only a small frequency band is removed from the spectrum. The analysis of the interaction of these pulses together with the results presented in [21–23] and [25] will give a detailed description of the photoassociation of ultracold molecules.

This paper is organized as follows. In section 2, we present the experimental set-up and introduce the different pulse shapes. The numerical methods which are used for the quantum dynamical calculations are presented in section 3. In section 4, the results are presented in the following way: first, we study the effect of a sharp high-pass filter in the frequency domain. Then we compare the effect of a spectrum which has its frequencies blue detuned to the atomic resonance to one with its components red detuned to the atomic D_1 resonance. A further spectral shape of the pump pulse was created by a modulation with a notch filter. The transients resulting from these resonant and non-resonant pulses are presented in the last part. In each case, the measurements are accompanied by quantum dynamical simulations. In section 5, we analyse the frequency of the transient oscillations. Finally, we discuss the effect of different pulse modulations and conclude at the end.

2. Experimental set-up

The femtosecond laser pulses are delivered by a regenerative amplifier (Coherent RegA 9050) seeded by a Mira oscillator. The pulses have an energy of 4 μJ at a repetition rate of 100 kHz. The central wavelength is tunable and set to 795 nm for experiments close to the D_1 line addressing the electronically excited $5s+5p_{1/2}$ state. In the measurements concerning the $5s+5p_{3/2}$ state at the D_2 line, the wavelength of the laser is centred at 785 nm. The FWHM amounts to 25 nm in both cases. The laser power is split into two parts: 10% are used for the pump pulse which is modulated. The modulation takes place in the Fourier plane of a 4f-line consisting of two gratings (2000 lines mm^{-1}) and two cylindrical lenses with a focal length of 250 mm. The frequency filtering is done by a physical block in the Fourier plane. For the high-pass filter we used a razor blade blocking all frequencies below the edge position. A needle of 1.6 mm in diameter acts as a notch filter and blocks a frequency band which is approximately 35 cm^{-1} wide. Both are mounted on a high-precision stage to change the cut-off frequency. The position of the cut-off is specified relative to the atomic resonance, which is determined by measuring the atomic fluorescence. This method gives the position of the atomic resonance and the cut-off position with a resolution of 1.8 cm^{-1}. In the case of the needle, the reference point is taken to be the lower frequency edge. While investigating transitions near the D_1 line, the frequencies of the atomic D_2 resonance and above (>12794.6 cm^{-1}) are removed by a fixed additional blocker to avoid disturbing the MOT by photon pressure and multi-photon ionization.

The major fraction of the laser power pumps a non-collinear optical parametric amplifier (NOPA) which delivers the ionization probe pulse. The wavelength of the probe pulses is centred around 490 nm with 25 nm spectral width. The probe pulses are not compressed yielding about 425 fs pulse duration and a pulse energy of 0.2 μJ. The pump and probe pulses are collinearly overlapped and focused in the trap with a lens of 300 mm focal length. The delay between the pump and probe

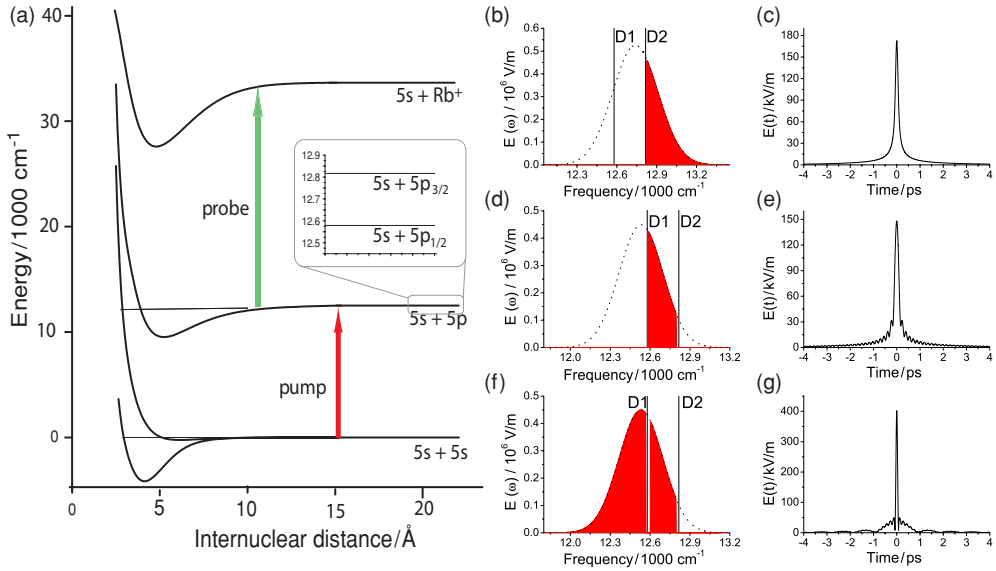

Figure 1. (a) Pump probe excitation scheme for rubidium. The pump pulse transfers population to the electronically excited state. The manifold of 5s+5p states have $5s+5p_{3/2}$ (D_2) and $5s+5p_{1/2}$ (D_1) as an asymptote. (b), (d) and (f) depict the spectral amplitude of the pulse before (dotted black line) and after removal of frequency components (red). The corresponding field in time is shown in (c), (e) and (g). (b) and (c) depict a pulse investigating the states at the $5s+5p_{3/2}$ (D_2) asymptote. A frequency high pass filter removes all frequencies below the cut-off position of +8 cm^{-1}, including the resonance. In (d), (e), (f) and (g) the pulse central frequency is set close to the D_1 resonance to investigate the states at the $5s+5p_{1/2}$ asymptote. In (d) and (e) a high pass filter with a cut-off position of +5 cm^{-1} is applied. In the pulse depicted in (f) and (g) a narrow frequency band of 35 cm^{-1} (from −12 to +23 cm^{-1}) is removed from the spectrum by a notch filter. In the two latter cases the atomic D_2 resonance is additionally removed. The uncut Gaussian spectrum is indicated by the dotted line.

pulse is variable and typically scanned between −5 ps and 10 ps.

As a sample, we capture about 10^8 Rb^{85} in a background vapour loaded MOT at temperatures of about 100 μK. The MOT is used in dark SPOT configuration which leads to densities of 10^{11} cm^{-3} whereof 90% are in the $F = 2$ hyperfine ground state. Atomic and molecular ions produced in the trap are extracted by a constant electrical field of 40 V cm^{-1}, mass selected by a quadrupole, and detected with single ion efficiency in a channeltron. A more detailed description of the set-up can be found in [22].

3. Numerical methods

In order to gain deeper insight into the excitation process, we theoretically study the interaction of the shaped laser pulse with a pair of ultracold colliding atoms. We numerically solve the time-dependent Schrödinger equation taking two electronic states into account. The ground state with diatomic potential V_g and the excited state with V_e are coupled by the time-dependent laser field $E(t)$ in the dipole and rotating wave approximations. The corresponding Hamiltonian reads

$$\hat{\mathbf{H}} = \begin{pmatrix} \hat{\mathbf{T}} + V_g(\hat{\mathbf{R}}) & \hat{\mu}E(t) \\ -\hat{\mu}E(t)^* & \hat{\mathbf{T}} + V_e(\hat{\mathbf{R}}) - \Delta \end{pmatrix}. \quad (1)$$

Here, Δ is the detuning of the pump pulse central frequency relative to the dissociation limit of the particular excited state. $\hat{\mathbf{T}}$ is the kinetic energy operator, $\hat{\mathbf{R}}$ is the internuclear distance and $\hat{\mu}$ is the transition dipole moment of the diatomic molecule. The electrical field of the pulse in time $E(t)$ is obtained by the Fourier transformation of the frequency modulated spectrum as described in [23]. To represent the wavefunctions and operators, a Fourier grid method with adaptive step size [26] is employed. The time evolution is achieved using the Chebyshev propagator [27]. This method has already been successfully applied to model the transients obtained for fs pulses shaped with different low-pass filters near the $5s+5p_{1/2}$ (D_1) and $5s+5p_{3/2}$ (D_2) asymptotes including linear chirps [23]. It was shown that the effect is only due to electronic dynamics. The propagation of a well-localized wave-packet could not be observed due to the very long round trip time and a very rapid dephasing in these high-lying states. The exact shape of the respective electronic state would only change the overall excitation rate due to the differing Franck–Condon factors. Therefore, the calculations are carried out exemplarily for two electronic states only. We start with a continuum scattering state of the $a^3\Sigma_u^+$ potential with a collision energy corresponding to 100 μK. The electronically excited molecular state is taken to be the 1_g potential for the states near the D_1 atomic resonance, and 0_g^- for the $5s+5p_{3/2}$ asymptote (D_2). The effect of the ionizing probe pulse is modelled by convoluting the transient by a normalized Gaussian of 425 fs FWHM. The measured data are fitted to the quantum dynamical simulations only by a single linear scaling factor.

4. Results and discussion

In this section, the pump probe results are presented along with the corresponding quantum dynamical simulations. The molecular potential energy scheme and the suggested pulse sequence are schematically shown in figure 1(a). A shaped

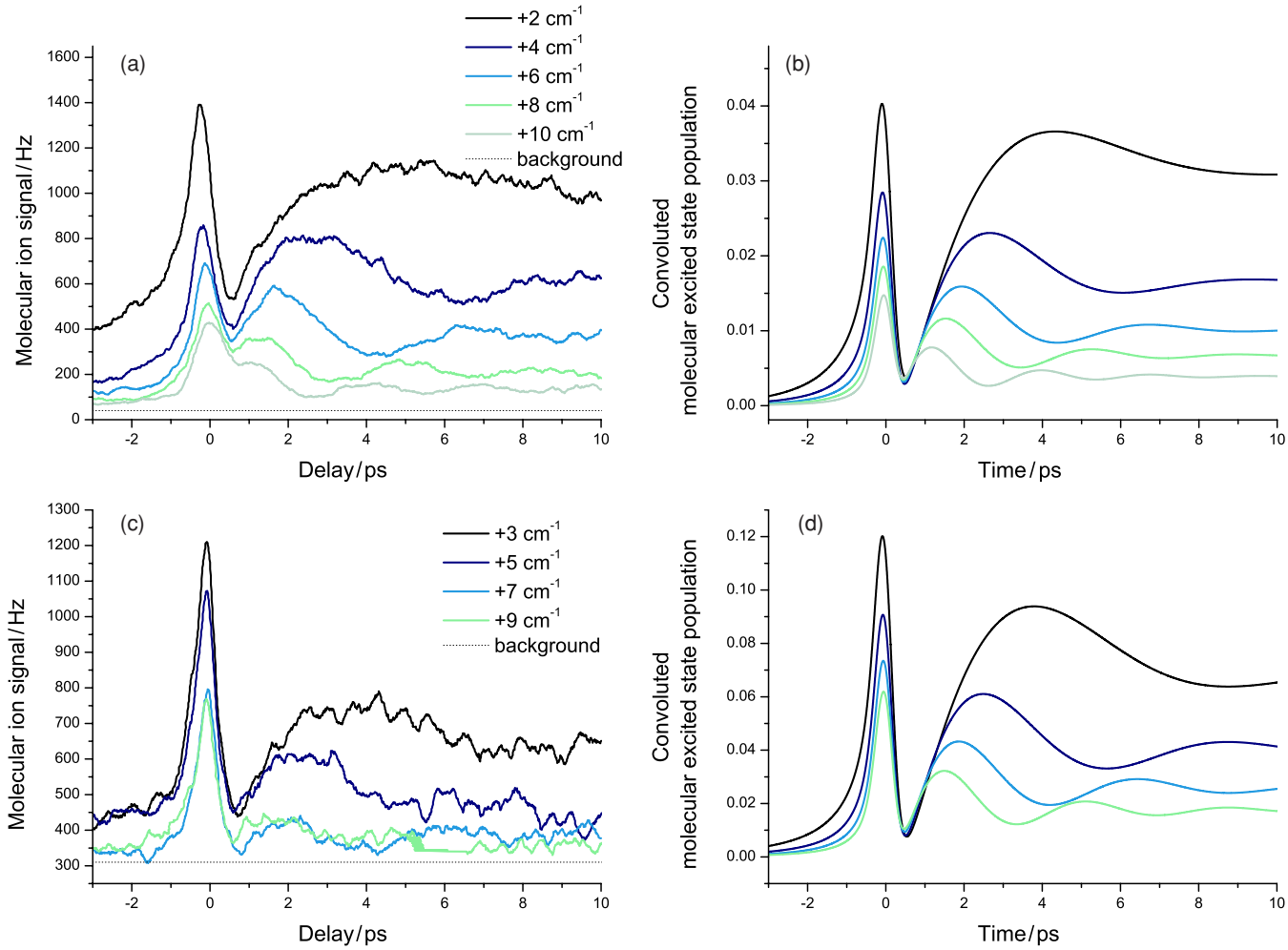

Figure 2. Measured pump probe transients obtained for a high pass filtered pump pulse with different cut-off positions near the $5s+5p_{3/2}$ (D_2) (a) and $5s+5p_{1/2}$ (D_1) asymptotes (c) are presented. Further, the simulated pump probe traces for the corresponding cut-off position near the atomic D_2 (b) and D_1 (d) resonances are shown.

pump pulse creates molecular population in the 5s+5p states. This population is transferred by a second pulse with variable time delay to an ionic state. The ions created by the probe pulse only arise from molecules produced by trap light and give a constant background signal which is indicated by a dashed line in all graphs.

4.1. Blue detuned pulses near the atomic D_1 and D_2 resonances

First, we discuss the transients resulting from a pulse modulated by a high-pass filter. The frequencies below the cut-off position, including the resonance, are removed yielding a pulse with its frequencies blue detuned to the atomic resonance. The cut-off position of the filter is given relative to the particular atomic resonance. We investigate the states belonging to the $5s+5p_{1/2}$ (D_1) and the $5s+5p_{3/2}$ (D_2) asymptote with separate pump pulses. In the case of the $5s+5p_{1/2}$ asymptote, we additionally remove the frequencies of the D_2 resonance and above from the spectrum. This allows us to suppress effects originating from the $5s+5p_{3/2}$ asymptote and to avoid disturbance of the MOT.

Two typical spectra of the pump pulse for the D_1 and D_2 lines are shown in figures 1(b) and (d), respectively. The corresponding pulses in time are lengthened by the frequency filtering, compared to the uncut pulse (depicted in figures 1(c) and (e)). In the case of the pulse investigating the states near the $5s+5p_{1/2}$ asymptote (D_1), where the spectral intensity is modulated with two sharp cuts (figure 1(d)), the pulse in a function of time features an oscillatory envelope (figure 1(e)).

The measured and calculated pump probe traces are depicted in figure 2. They look very similar to pulses near the D_1 and D_2 resonances and can be divided into three characteristic parts. For negative time delays, when the probe pulse precedes the shaped pump pulse a constant ion count rate is obtained. At zero delay, the signal exhibits a peak. After this peak, at positive time delays, the signal increases and shows modulations which decrease in amplitude. The frequency of the oscillation is directly proportional to the detuning of the cut-off position from the atomic resonance, as was the case in [21]. The first minimum at about 0.35 ps is independent of the cut-off position. The average ion signal at positive delays is larger than at negative delays. The detected molecular ion rate at positive delays divided by the rate detected at negative

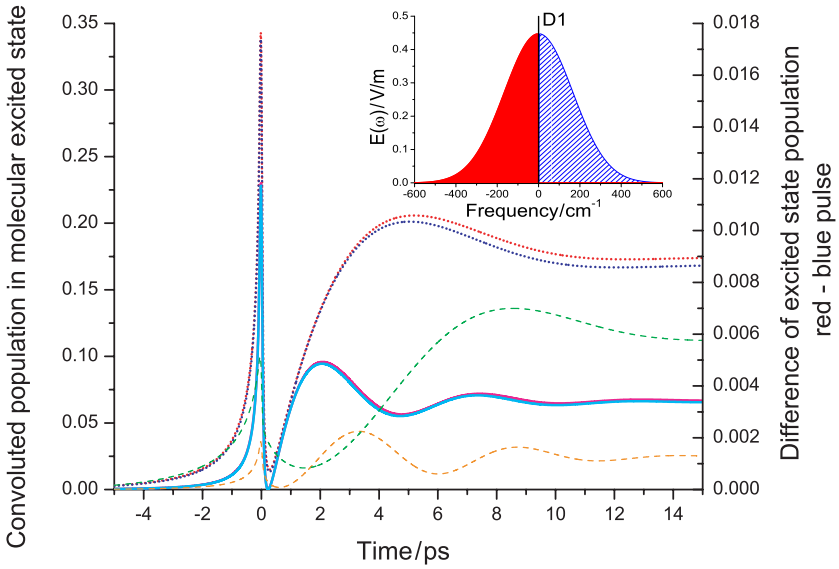

Figure 3. Transients resulting from a pump pulse with its frequency components red to the resonance (red and magenta) and blue to the resonance (blue and cyan). The cut-off positions were symmetric and chosen to be ± 2 cm^{-1} (solid) and ± 6 cm^{-1} (dashed). The curves for the pulse which encloses the frequencies above resonance are printed in blue and cyan. The colour of the transients resulting from pulses with the frequencies below the resonance is red and magenta. The difference in population of each transient pair is also depicted in dashed green (± 2 cm^{-1}) and dashed orange (± 6 cm^{-1}) on a separate scale. The spectra are chosen to be symmetric around the D_1 resonance (see the inset).

delays is found to be constant as the cut-off position is varied. Both are decreasing with the detuning of the cut-off position of the frequency filter. The cut-off positions for larger detunings remove the more important frequencies close to the resonance of the pulse which result in a lower overall ion signal.

The physical processes which lead to these transients can be explained by a driven dipole. The high peak power of the pump pulse causes nonlinear processes, which have to be considered in the interactions between the light field and the atom pair. Population accumulates in the vibrational states just below the asymptote of the first excited state creating a dipole. This induced optical dipole oscillates with its intrinsic frequency and coherently exchanges energy with the declining field. The instantaneous frequency of the temporal field is equal to the cut-off position in the spectrum. This results in a beating where the modulation exactly matches the cut-off detuning. A detailed analysis of these transients can be found in [23] and [28].

The constant ion signal at negative delays is not reproduced by our theoretical calculations, since we only consider the interaction with one single pulse. The signal at negative delays most likely originates from molecules which were photoassociated by a preceding pulse and have spontaneously decayed to the ground state. These are detected by near resonant ionization via intermediate states below the 5s+5d asymptote. A complete analysis of the photoassociation process along with further supporting experiments is described in [22].

The measurements near the $5s+5p_{1/2}$ (D_1) and the $5s+5p_{3/2}$ (D_2) resonance slightly differ regarding their absolute ion signal. It is higher for the D_2 resonance, which is mainly due to the larger dipole transition moment and differences in the spectral intensity distribution. The difference in the spectral intensity distribution could be caused by a deviation in pulse energy, central wavelength, spectral width, or a second cut which is needed to remove the atomic resonance that is not under investigation.

4.2. Blue versus red detuned pulses

The transients shown in figure 2 are similar to those produced by pulses which have their spectral intensity below the atomic resonance [21–23]. In this section, we investigate the difference in the transients obtained by pulses having the spectral intensity blue and red detuned respective to the atomic resonance. For this investigation, this effect has to be separated from a variation of pulse parameters which can only be done in a theoretical analysis. The main parameters which affect the transients are the position of the spectral cut-off and the power of the pump pulse. A tiny difference between these pulses having their spectral intensity on the blue or red side of the atomic resonance cannot be experimentally resolved. For a detailed comparison of the transients obtained by these different pulse types, we therefore generated a set of simulations. In these simulations, we choose the pulse parameters in such a way that the spectral intensity distribution for the pulses with their spectral intensity on the blue side is the mirror image of the pulses which have their spectral intensity on the red side of the resonance (see the inset of figure 3). The position of the cut-off frequency is negative for the pulses which have their frequencies below the resonance and positive for those with their frequencies above. In both cases, the resonance is not enclosed in the spectrum. The states corresponding to the $5s+5p_{3/2}$ (D_2) asymptote were not taken into account.

The molecular transients for a cut-off position of 2 cm^{-1} and 6 cm^{-1} are depicted in figure 3. The overall transients for

a pulse which has its frequency components on the blue side (cut-off position of +2 and +6 cm^{-1}) of the resonance look similar to those obtained with a pulse where the frequencies are situated on the red side (cut-off position of −2 and −6 cm^{-1}). In a closer look, one observes that the population in the bound levels of the excited state is larger for the pulse with its spectral intensity red to the resonance. The difference in molecular population is decreasing with the cut-off position. The variation of the difference over time is similar to the transients itself, but shifted by a quarter period of the oscillation.

To investigate the differences in the transients, we analyse the vibrational distributions of the population in the excited state after interaction with the pulse. Figure 4 compares the vibrational distributions in the excited state for pulses with their spectral intensity on the blue or red side of the atomic resonance. The detuning of the spectral cut-off position amounts in both cases to 2 cm^{-1} from the atomic resonance. The major fraction of the population in the molecular excited state accumulates in the vibrational levels from $v = 250$ to 271 very close (bound by less than 2 cm^{-1}) to the resonance. These states cannot resonantly be addressed by one of the frequency modulated pulses. Therefore, this population must be created due to the high peak intensity of the pump pulse. Nonlinear effects such as power broadening, Stark shift and Rabi cycling become relevant and can non-resonantly create population in these levels. The difference in population is mainly localized in the vibrational states v = 200–246. This fraction of the excited state population is more deeply bound than the major part of the molecular population. These vibrational states cannot resonantly be populated by the pulse which has spectral components on the red side of the resonance (see figure 4). The pulse with its frequency components blue detuned to the resonance has no overlap with any bound molecular state. This portion of molecules which is additionally produced by the red detuned pulse amounts to only 3% of the total population. The population difference in these states can be explained by their binding energy. The binding energy of the vibrational state $v = 220$, where the difference in molecular population has its maximum, is −0.7487 cm^{-1}. For this state, the effective detuning consists of the actual detuning and the binding energy. In the case of the pulse with the frequency components blue detuned to the resonance the detuning gets larger. For the pulse with its frequency components red detuned to the resonance it gets smaller. The molecular rate is decreasing with larger detunings for both types of spectra (cf figure 2). The shift is relatively larger for small detunings. Therefore, the difference is getting larger when the cut position is closer to resonance. For higher vibrational levels ($v > 247$) the binding energy is smaller than 10^{-7} cm^{-1} and the shift has almost no effect [5]. For vibrational levels below $v = 200$, the Franck–Condon factors get too small for an efficient population. For the major part of photoassociated molecules, it does not matter if the spectral intensity is situated above or below the atomic resonances.

[5] It is not entirely clear what the minimal binding energy is for the direct detection of a molecule in a mass spectrometer.

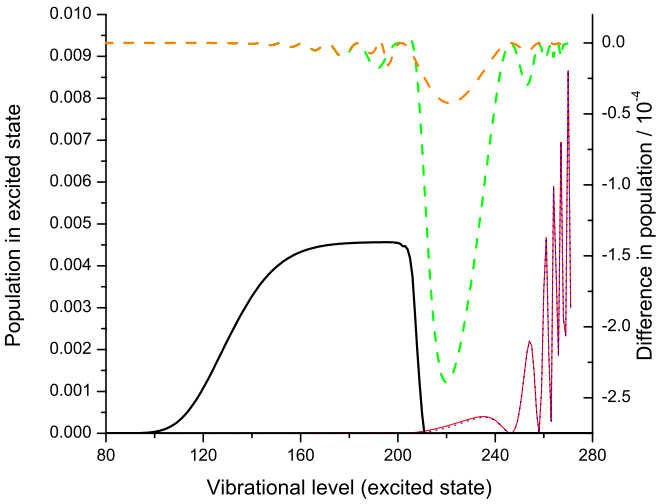

Figure 4. The vibrational distribution of the excited state molecules after the interaction with the frequency modulated pump pulse. The cut-off position in the case of the high pass filter is +2 cm^{-1} yielding the blue frequency components (blue dotted line). For the low pass filter it is set to −2 cm^{-1} (red line). The difference in the population between high pass and low pass filtered pulses is shown for a cut-off position of ±2 and ±6 cm^{-1} (green dashed line and orange dashed line). The spectrum of the blue cut pulse (−2 cm^{-1}) is provided to put it in relation with the frequency domain (black line).

4.3. Modulation with a band filter

The previous section has shown that pulses with a spectral intensity red or blue detuned to the atomic resonance cause the same process. The resulting coherent transients in the free-bound transition of a colliding atom pair are very similar. From there it seems to be logical to use both frequency components of the pulse, situated on the blue and red side of the atomic resonance, simultaneously. Such a pulse covers nearly twice the frequency components which should lead to an increase of controllability. This combination of blue and red frequencies results in a nearly Gaussian spectral distribution with a dip at the atomic resonance. This dip is again necessary to avoid perturbation of the trap and is created by a needle in the Fourier plane of the shaper. A spectrum of this type of pump pulse is shown in figure 1(f) investigating the states of the $5s+5p_{1/2}$ asymptote. Since the experiments and simulations have shown that the transients do not depend on the characteristics of the states belonging to the $5s+5p_{1/2}$ (D_1) or $5s+5p_{3/2}$ (D_2) asymptote, we present exemplary experiments near the atomic D_1 resonance only.

The transients of five different filter positions along with quantum dynamical simulations are depicted in figure 5. The first three graphs of figure 5, (a)–(c), show transients resulting from a pump pulse where the D_1 resonance is blocked by the needle. In figures 5(d) and (e) the transients result from a pulse where the atomic resonance is enclosed in the spectrum. In (d) the frequency filter is situated below the D_1 resonance whereas in (e) it blocks a frequency band above.

The transients obtained by all these pump pulses are similar to those where the frequencies above or below the resonance are blocked. One additional feature is observed: the

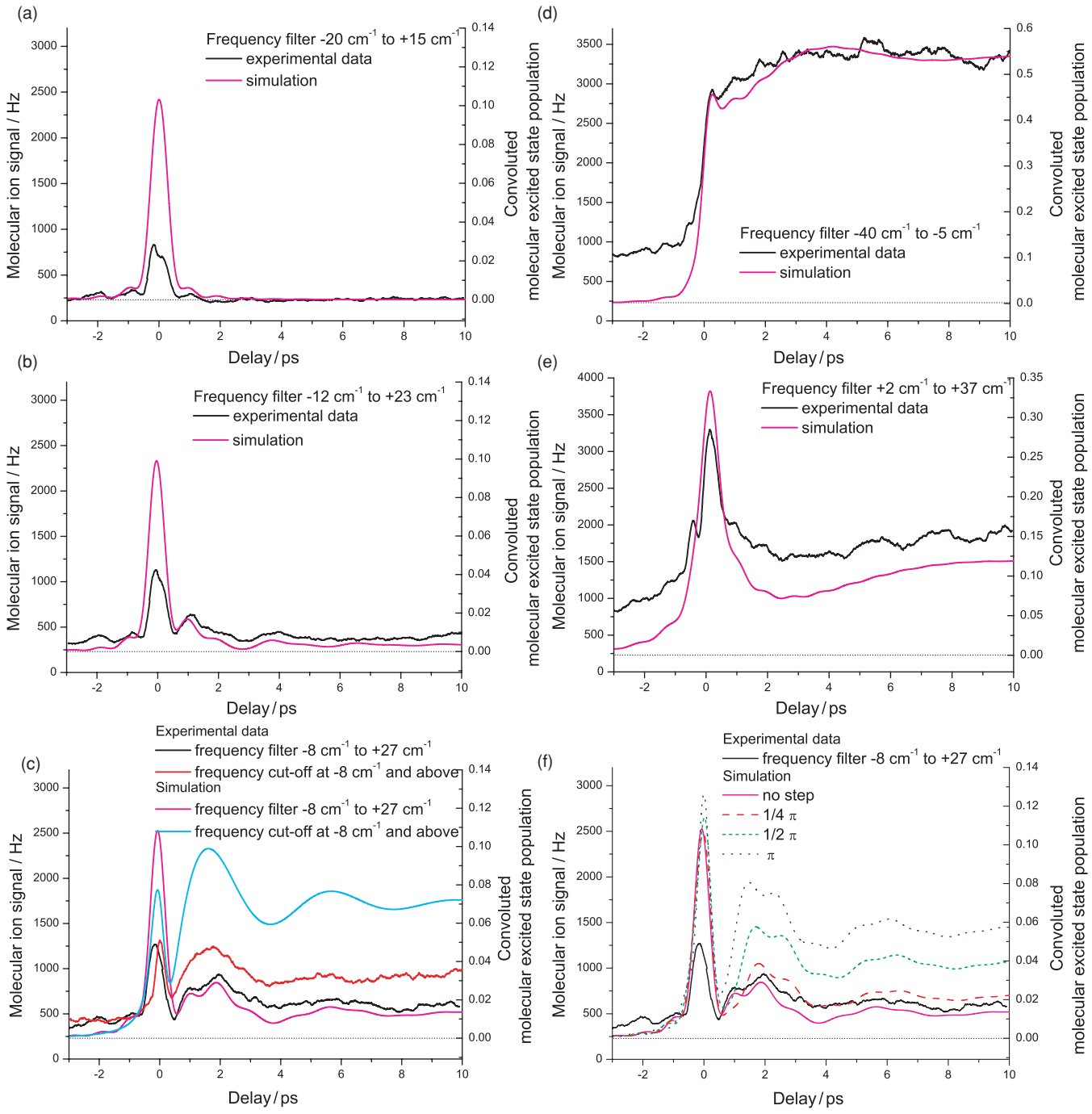

Figure 5. Measured pump probe transients and the corresponding calculations for different needle positions at the $5s+5p_{1/2}$ (D_1) asymptote. In (a)–(c) we show the transients which were produced by a non-resonant pump pulse. In (c) a second pair of curves is presented where additionally to the notch filter the spectral intensity below the notch filter is removed. Transients and simulations for pump pulses with the resonance enclosed are shown in (d) and (e). In (d) the needle blocks frequencies situated below the atomic D_1 resonance (-40 cm^{-1} to -5 cm^{-1}). (e) shows the other case where the needle blocks a frequency band above the atomic D_1 resonance (+2 cm^{-1} to +37 cm^{-1}). The background signal is indicated by a black dotted line. The resonant pulses perturb the trap, therefore the scaling between experimental data and the quantum dynamical simulations is changed. In (f) the effect of a spectral phase step located at the resonance is demonstrated. The frequency filter position is kept constant blocking a frequency band from -8 cm^{-1} to +27cm^{-1} like in (c). The simulations for step heights of $1/4\pi$, $1/2\pi$ and π are compared to that with a flat phase. The position of the phase step set to resonance.

ion signal at positive delay is modulated by a second higher frequency. This frequency can be attributed to the second cut-off in the spectrum. The slow oscillation is due to the frequency cut-off close to the resonance, e.g. at -8 cm^{-1} in figure 5(c). The transient of a pulse with the same cut-off position (-8 cm^{-1}) having its spectral components on the red side of the resonance is also depicted (turquoise line). This transient has the same long oscillation period due to the same

frequency cut-off. The faster second oscillation is expected to arise from the second cut-off in the spectrum obtained by a pulse which is frequency modulated by the notch filter (at +27 cm^{-1}). Since this cut-off is further detuned from the resonance, this oscillation is faster. A detailed quantitative analysis of the modulation frequencies is presented below.

The population in the excited state depends on the position of the blocked frequency band. When the frequency components from -20 cm^{-1} to +15 cm^{-1} are blocked (figure 5(a)) almost no molecular population remains in the excited state after the pulse is over. Going to the filter position of -12 cm^{-1} to +23 cm^{-1} (figure 5(b)) the number of created molecules rises, and when the needle blocks the frequencies from -8 cm^{-1} to +27 cm^{-1} (figure 5(c)) the population is even larger. The two modulations in the transient, which are due the two cuts in the spectrum, can be clearly observed. The long oscillation as well as the faster one on top shows an excellent agreement with the calculated population.

The transients resulting from pulses which consist of red and blue frequency components compared to pulses which provide only the red frequency components differ in the ion signal. The peak at zero time delay is higher in the case of the band filter which can be attributed to the higher peak power of the electric field. The ion signal at positive delays produced by the pulses containing both frequency components, red and blue to the resonance, is smaller although these pulses provide a higher spectral intensity. This difference can be explained by destructive interference of the red and blue frequencies, which is sensitive to the relative phase of these components [29]. To confirm this interference effect, we theoretically investigate the transients by applying a step function to the spectral phase. The position of the phase step was set to the resonance. The calculations for different heights of the step for the band filter blocking the frequencies from -8 cm^{-1} to +27 cm^{-1} are depicted in figure 5(f). The transient signal increases with the step height and becomes maximal for a step height of π. Furthermore, the phase of the faster oscillation is shifted by this phase step modulation. The good agreement of the experimental results with the simulation without phase step shows that the spectral phase of the experimentally used pulses is indeed flat.

Transients where the resonance is enclosed in the spectrum of the pump pulse are shown in figures 5(d) and (e). For the band filter blocking the frequencies from +2 cm^{-1} to +37 cm^{-1} (figure 5(e)) the resonance is just in the spectrum, and the pump probe signal shows a peak in the molecular population at zero delay dropping down to half for positive delays.

In the case shown in figure 5(d), the needle blocks a band of frequencies from -40 cm^{-1} to -5 cm^{-1} which is below the atomic D_1 resonance. This transient shows a steep increase of the molecular population which remains on a high level when the pulse is gone. In both cases, the transients with the two oscillations can be reproduced by theory.

The scaling between theory and experimental data has to be changed compared to the non-resonant case. In the resonant case (figures 5(d) and (e)), photon pressure and atomic multiphoton ionization have an impact on the ultracold ensemble. The density is reduced and the initial-state distribution of the atoms is changed. This is not taken into account in the simulations. The real number of molecules which can be created by a pulse depends on the number of atoms present in the focus of the pump pulse and the distribution of the spectral intensity. There is a tradeoff between having frequencies very close to the resonance in the pump pulse and perturbation of the trapped ensemble.

5. Frequency analysis

If more than one cut is applied to the pulse spectrum, additional modulations are observed in the oscillation of the excited state population. We analyse the effect of a second and a third cut-off position. We choose the transients at the atomic D_1 resonance obtained with a blue detuned pulse of the type depicted in figure 1(d) to serve as an example for two cuts in the spectrum. The transients obtained by the pulse which is modulated by a notch filter provide the basis for an analysis of three cuts in the spectral domain which is shown in figure 1(f). Since the excited state oscillations are caused by the interaction of the molecular dipole with the field, the modulations are expected to reflect a beating of the frequency of the created dipole with two or more cut frequencies as was shown in [23]. The depth of the modulations is expected to be due to the relative phase between the beat frequencies. In order to extract the frequency and amplitude of the additional modulations, a spectral analysis is performed on the calculated transients. We used the filter diagonalization method [30, 31] which allows us to extract spectral information from very few oscillation periods. The signal is decomposed into a sum of decaying exponentials, $C(t) = \sum_k d_k e^{-i\omega_k t - \Gamma_k t}$, and the frequencies ω_k, decay rates Γ_k, and complex amplitudes d_k are extracted from the signal. Two periods of the data sets which are in between the arrows shown in figures 6(a), (d) and (g) are used. The analysed data are presented in three parts: the transients are accompanied by the associated spectrum including the weights of the dominating frequency components and the corresponding lifetimes ($|\Gamma_k|^{-1}$).

The first example depicted in figures 6(a)–(c) shows the case of two cut-off positions in the spectrum. One cut-off position is kept constant removing frequencies which are further than +216 cm^{-1} detuned from the atomic D_1 resonance to remove the D_2 resonance. The other cut-off position is situated at +5 cm^{-1} (black line) and +9 cm^{-1} (blue dashed line) (cf figure 1(d)).

The absolute spectral weights $|d_k|$ of the dominating frequencies ω_k are shown in figure 6(b). The zero frequency component of the spectrum gives a constant offset to the oscillations. The cut-off positions $\omega = 9$ cm^{-1} (black line) and $\omega = 5$ cm^{-1} (blue dashed line) as well as the difference of the two cut-off positions $\omega = 207$ cm^{-1} (black line), $\omega = 211$ cm^{-1} (blue dashed line) appear in the spectra. Besides these components, unexpected frequencies such as $\omega = 6.5$ cm^{-1}, $\omega = 211.7$ cm^{-1} (black lines) or $\omega = 6.2$ cm^{-1}, $\omega = 217.3$ cm^{-1} (blue dashed lines) are also observed.

In order to interpret these additional lines, the lifetimes of the corresponding frequencies are examined and shown in

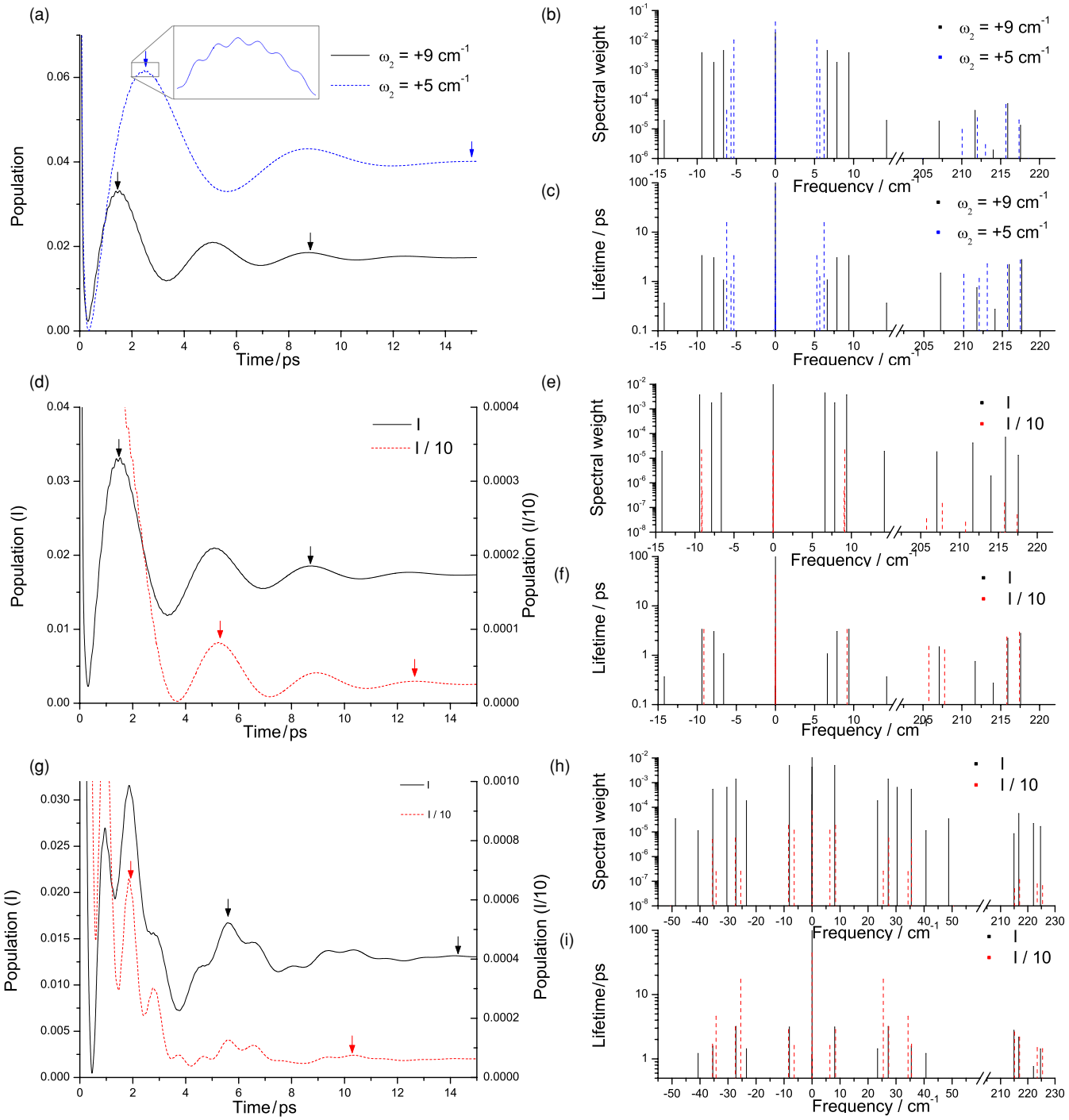

Figure 6. Frequency analysis of the transient oscillations for experiments near the D_1 resonance. (a) depicts the transients obtained by setting the cut-off position to +216 cm^{-1} and having a second cut-off position at +5 cm^{-1} (black line) and +9 cm^{-1} (blue dashed line) (cf figure 1(b)). (b) shows the absolute spectral weights of the dominating frequencies. In (c) the corresponding lifetimes are shown. In (d)–(f) the effect of the pump pulse intensity is investigated for the two cut-off positions of +5 cm^{-1} and +216 cm^{-1}. Figure (d) shows transient population, (e) the frequency spectrum and (f) the corresponding lifetimes. In (g)–(i) the transients of a pulse whose spectrum exhibits three cut-off positions, as in figure 1(f), are studied. The graphs corresponding to the originally used intensity are represented by black lines. The graphs where the intensity is reduced to 10% are represented by red dashed lines.

figure 6(c). Each frequency corresponding to a cut-off position or to the difference of cut-off positions has significantly larger lifetimes than the other frequencies in the spectrum (note the logarithmic scale). The frequencies with short lifetimes are most effective at time $t = 0$ where the pulse is still strong. This indicates that the unexpected lines are caused by the interaction between the molecules and the strong field during the main peak of the pulse. In order to understand the intensity dependence of the unexpected lines, the same spectral analysis is performed for two different intensities: the intensity which was used for the calculations above (I, black line) and a tenth of this intensity (I/10, red dashed line). For

this analysis the cut-off positions are set to +216 cm^{-1} and +5 cm^{-1}, as in the example before. The results are shown in figures 6(d)–(f).

An analogous analysis is performed for three cut-off positions which corresponds to a spectral intensity distribution shown in figure 1. The first cut-off is situated at +216 cm^{-1}, the second is set to -8 cm^{-1} and the third cut-off is set to +27 cm^{-1} with respect to the D_1 resonance (figures 6(g)–(i)).

For higher intensity, a splitting of the frequencies around the cut-off positions as well as around the difference of the cut-off positions is observed. Moreover, unexpected lines with large spectral weight are observed, cf figures 6(e) and (h). For a lower intensity, these unexpected lines disappear. The frequency components at the cut-off positions and the difference of the cut-off positions show a large, symmetric splitting. The strong intensity dependence of the components with short lifetimes confirms further that they are caused by the strong interaction near the pulse maximum.

6. Conclusion

We have examined the off-resonant population of bound molecular states outside the perturbative regime. We have discussed transients where the pump pulses are blue detuned with respect to the atomic resonance. The transients are well described by our theoretical calculations. They show by and large the same effect as red detuned pulses. The reason for the similar behaviour can be attributed to the high peak intensity of the pump pulse. Due to nonlinear effects, population is transferred non-resonantly to the excited state. Therefore, it is basically irrelevant whether the spectral intensity is situated below or above the resonance. Small differences occur due to transitions to bound states with binding energies of about 0.7 cm^{-1}. The transient behaviour was further investigated with pulses where the spectral intensity is nearly Gaussian and only a band around the resonance is removed. These nearly transform limited pulses have a higher peak intensity and yield very similar transients compared to red and blue detuned pulses. In this case, the transient is determined by interference of the red and blue frequency components, which was confirmed by calculations with phase modulations. The analysis of the vibrational distribution in the molecular excited state shows that the most important frequencies for the photoassociation and the transients are very close to resonance. The instantaneous frequency is the major parameter in this process and is directly connected to the cut position. The spectral cut positions respective to the resonance can directly be connected to the oscillation of the transient, which was confirmed by frequency analysis. The total number of photoassociated molecules is a tradeoff between having frequencies close to the atomic resonance within the pulse and the perturbation of the atomic density. These experiments with blue detuned pulses reveal that in femtosecond photoassociation the details of the molecular structure are less important than in cw photoassociation. Here, this is due to the strong field effect interpreted by transient electronic excitation.

Acknowledgments

This work was supported by the Deutsche Forschungsgemeinschaft in the framework of SFB 450, SPP 1116, and the Emmy Noether program.

References

[1] Phillips W D 1998 Laser cooling and trapping of neutral atoms *Rev. Mod. Phys.* **70** 721–41
[2] Chu S 2002 Cold atoms and quantum control *Nature* **416** 206–10
[3] Weinstein J D, de Carvalho R, Guillet T, Friedrich B and Doyle J M 1998 Magnetic trapping of calcium monohydride molecules at millikelvin temperatures *Nature* **395** 148–50
[4] Bethlem H L, Berden G and Meijer G 1999 Decelerating neutral dipolar molecules *Phys. Rev. Lett.* **83** 1558
[5] Köhler T, Góral K and Julienne P S 2006 Production of cold molecules via magnetically tunable feshbach resonances *Rev. Mod. Phys.* **78** 1311
[6] Jones K M, Tiesinga E, Lett P D and Julienne P S 2006 Ultracold photoassociation spectroscopy: long-range molecules and atomic scattering *Rev. Mod. Phys.* **78** 483
[7] Koch C P, Palao J P, Kosloff R and Masnou-Seeuws F 2004 Stabilization of ultracold molecules using optimal control theory *Phys. Rev.* A **70** 013402
[8] Luc-Koenig E, Kosloff R, Masnou-Seeuws F and Vatasescu M 2004 Photoassociation of cold atoms with chirped laser pulses: time-dependent calculations and analysis of the adiabatic transfer within a two-state model *Phys. Rev.* A **70** 033414
[9] Koch C P, Kosloff R and Masnou-Seeuws F 2006 Short-pulse photoassociation in rubidium below the D_1 line *Phys. Rev.* A **73** 043409
[10] Judson R S and Rabitz H 1992 Teaching lasers to control molecules *Phys. Rev. Lett.* **68** 1500
[11] Lindinger A, Lupulescu C, Plewicki M, Vetter F, Merli A, Weber S M and Wöste L 2004 Isotope selective ionization by optimal control using shaped femtosecond laser pulses *Phys. Rev. Lett.* **93** 033001
[12] Levis R J, Menkir G M and Rabitz H 2001 Selective bond dissociation and rearrangement with optimally tailored, strong-field laser pulses *Science* **292** 709–13
[13] Vogt G, Krampert G, Niklaus P, Nuernberger P and Gerber G 2005 Optimal control of photoisomerization *Phys. Rev. Lett.* **94** 068305
[14] Fatemi F, Jones K M, Wang He, Walmsley I and Lett P D 2001 Dynamics of photoinduced collisions of cold atoms probed with picosecond laser pulses *Phys. Rev.* A **64** 033421
[15] Wright M J, Gensemer S D, Vala J, Kosloff R and Gould P L 2005 Control of ultracold collisions with frequency-chirped light *Phys. Rev. Lett.* **95** 063001
[16] Brown B L, Dicks A J and Walmsley I A 2006 Coherent control of ultracold molecule dynamics in a magneto-optical trap by use of chirped femtosecond laser pulses *Phys. Rev. Lett.* **96** 173002
[17] Salzmann W *et al* 2006 Coherent control with shaped femtosecond laser pulses applied to ultracold molecules *Phys. Rev.* A **73** 023414
[18] Weise F *et al* 2007 Optimal control of multiphoton ionization of Rb_2 molecules in a magneto-optical trap *Phys. Rev.* A **76** 063404
[19] Viteau M, Chotia A, Allegrini M, Bouloufa N, Dulieu O, Comparat D and Pillet P 2008 Optical pumping and vibrational cooling of molecules *Science* **321** 232

[20] Viteau M, Chotia A, Allegrini M, Bouloufa N, Dulieu O, Comparat D and Pillet P 2009 Efficient formation of deeply bound ultracold molecules probed by broadband detection *Phys. Rev.* A **79** 021402
[21] Salzmann W *et al* 2008 Coherent transients in the femtosecond photoassociation of ultracold molecules *Phys. Rev. Lett.* **100** 233003
[22] Salzmann W *et al* 2009 Photoassociation and coherent transient dynamics in the interaction of ultracold rubidium atoms with shaped femtosecond pulses: I. Experiment arXiv:0903.4549
[23] Merli A *et al* 2009 Photoassociation and coherent transient dynamics in the interaction of ultracold rubidium atoms with shaped femtosecond pulses: II. Theory arXiv:0903.4401
[24] McCabe D J, England D G, Martay H E L, Friedman M E, Petrovic J, Dimova E, Chatel Béatrice and Walmsley I A 2009 Pump-probe study of the formation of rubidium molecules by ultrafast photoassociation of ultracold atoms *Phys. Rev.* A **80** 033404
[25] Eimer F *et al* 2009 Spectrally resolved coherent transient signal for ultracold rubidium molecules *Eur. Phys. J.* D **54** 711–4
[26] Kokoouline V, Dulieu O, Kosloff R and Masnou-Seeuws F 1999 Mapped Fourier methods for long-range molecules: application to perturbations in the $Rb_2(0_u^+)$ photoassociation spectrum *J. Chem. Phys.* **110** 9865–76
[27] Kosloff R 1988 Time-dependent quantum-mechanical methods for molecular dynamics *J. Phys. Chem.* **92** 2087–100
[28] Albert M, Mullins T, Götz S, Salzmann W, Wester R and Weidemülller M 2008 The interaction of a spectrally cut laser-pulse with a two-level atom *J. Mod. Opt.* **55** 3359–68
[29] Dudovich N, Oron D and Silberberg Y 2002 Coherent transient enhancement of optically induced resonant transitions *Phys. Rev. Lett.* **88** 123004–123004
[30] Neuhauser D 1990 Bound state eigenfunctions from wave packets: time–energy resolution *J. Chem. Phys.* **93** 2611–6
[31] Mandelshtam V A and Taylor Howard S 1997 Harmonic inversion of time signals and its applications *J. Chem. Phys.* **107** 6756–69